Distribution-Aware Coordinate Representation for Human Pose Estimation

Feng Zhang[1]   Xiatian Zhu[2]   Hanbin Dai[3]   Mao Ye[1]   Ce Zhu[4]

[1]School of Computer Science and Engineering, University of Electronic Science and Technology of China

[2]Centre for Vision, Speech and Signal Processing, University of Surrey

[3]School of Automation Engineering, University of Electronic Science and Technology of China

[4]School of Information and Communication Engineering, University of Electronic Science and Technology of China

{zhangfengwcy,daihanbin.ac,cvlab.uestc}@gmail.com,xiatian.zhu@surrey.ac.uk,eczhu@uestc.edu.cn

Abstract

While being the de facto *standard coordinate representation for human pose estimation,* heatmap *has not been investigated in-depth. This work fills this gap. For the first time, we find that the process of* decoding *the predicted heatmaps into the final joint coordinates in the original image space is* surprisingly significant *for the performance. We further probe the design limitations of the standard coordinate decoding method, and propose a more principled distribution-aware decoding method. Also, we improve the standard co-ordinate* encoding *process (i.e. transforming ground-truth coordinates to heatmaps) by generating unbiased/accurate heatmaps. Taking the two together, we formulate a novel* Distribution-Aware coordinate Representation of Keypoints *(DARK) method. Serving as a model-agnostic plug-in, DARK brings about significant performance boost to existing human pose estimation models. Extensive experiments show that DARK yields the best results on two common benchmarks, MPII and COCO. Besides, DARK achieves the 2nd place entry in the ICCV 2019 COCO Keypoints Challenge. The code is available online [36].*

1. Introduction

Human pose estimation is a fundamental computer vision problem that aims to detect the *spatial location* (*i.e. coordinate*) of human body joints in unconstrained images [1]. It is a non-trivial task as the appearance of body joints vary dramatically due to diverse styles of clothes, arbitrary occlusion, and unconstrained background contexts, whilst it is needed to identify the *fine-grained* joint coordinates. As strong image processing models, convolutional neural networks (CNNs) excel at this task [15]. Existing works typically focus on designing the CNN architecture tailored particularly for human pose inference [20, 25].

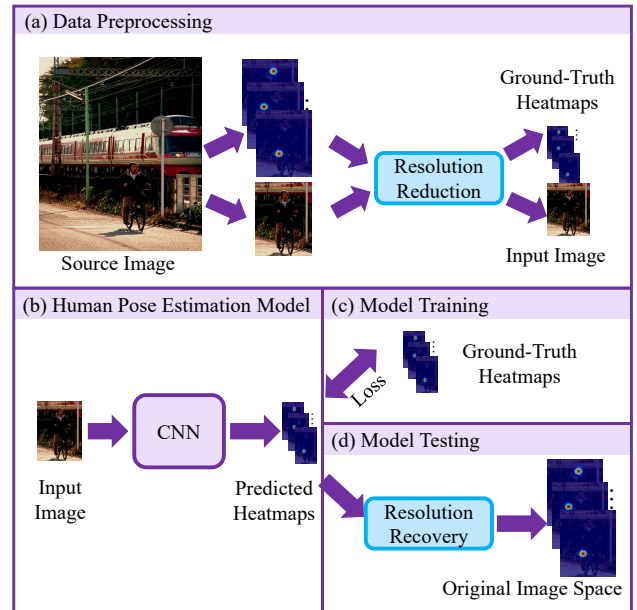Analogous to the common *one-hot vectors* as the object

Figure 1. Pipeline of a human pose estimation system. For efficiency, *resolution reduction* is often applied on the original person detection bounding boxes as well as the ground-truth heatmap supervision. So, the model operates in a low-resolution image space which reduces model inference cost significantly. At test time, a corresponding *resolution recovery* is therefore necessary in order to obtain the joint coordinate prediction in the original image space.

class label representation in image classification, a human pose CNN model also requires a ***label representation*** for encoding the *body joint coordinate labels*, so that the supervised learning loss can be quantified and computed during training and the joint coordinates can be inferred properly[1]. The *de facto* standard label representation is *coordi-*

---

[1]The *label representation* is for encoding the label annotations (*e.g.* 1,000 one-hot vectors for 1,000 object class labels in ImageNet), totally different from the *data representation* for encoding the data samples

nate heatmap, generated as a 2-dimensional Gaussian distribution/kernel centred at the labelled coordinate of each joint [30]. It is obtained from a ***coordinate encoding*** process, *from coordinate to heatmap*. Heatmap is characterised by giving spatial support around the ground-truth location, considering not only the contextual clues but also the inherent target position ambiguity. Importantly, this may effectively reduce the model overfitting risk in training, in a similar spirit of the class label smoothing regularisation [28]. The state-of-the-art pose methods [20, 33, 25, 38] are based on the heatmap coordinate representation.

With the heatmap label representation, one major obstacle is that, the computational cost is a *quadratic* function of *the input image resolution*, preventing the CNN models from processing the typically *high-resolution* raw imagery data. To be computationally affordable, a standard strategy (see Fig. 1) is to downsample all the person bounding box images at arbitrarily large resolutions into a prefixed small resolution with a data preprocessing procedure, before being fed into a human pose estimation model. Aiming to predict the joint location in the *original* image coordinate space, after the heatmap prediction a corresponding *resolution recovery* is required for transforming back to the original coordinate space. The final prediction is considered as the location with the maximal activation. We call this process as ***coordinate decoding***, *from heatmap to coordinate*. It is worthy noting that quantisation error can be introduced during the above resolution reduction. To alleviate this problem, during the existing coordinate decoding process a hand-crafted shifting operation is usually performed according to the direction from the highest activation to the second highest activation [20].

Despite being indispensable in model inference, the problem of coordinate encoding and decoding (*i.e.* denoted as *coordinate representation*) gains little attention. In contrast to the current research focus on designing more effective CNN structures, we reveal a *surprisingly* important role the coordinate representation plays on the model performance, much more significant than expected. For instance, with the state-of-the-art model HRNet-W32 [25], the aforementioned shifting operation of coordinate encoding brings as high as 5.7% AP on the challenging COCO validation set (Table 1). It is noteworthy to mention that, this gain is already much more significant than those by most individual art methods. But it is never well noticed and carefully investigated in the literature to our best knowledge.

Contrary to the existing human pose estimation studies, in this work we dedicatedly investigate the problem of joint coordinate representation including encoding and decoding. Moreover, we recognise that the heatmap resolution is one major obstacle that prevents the use of smaller input resolution for faster model inference. When decreasing the

---

(*e.g.* the object images from ImageNet).

input resolution from 256×192 to 128×96, the model performance of HRNet-W32 drops significantly from 74.4% to 66.9% on the COCO validation set, although the model inference cost falls from 7.1×10^9 to 1.8×10^9 FLOPs.

In light of the discovered significance of coordinate representation, we conduct in-depth investigation and recognise that one key limitation lies in the coordinate decoding process. Whilst existing standard shifting operation has shown to be effective as found in this study, we propose a principled distribution-aware representation method for more accurate joint localisation at sub-pixel accuracy. Specifically, it is designed to comprehensively account for the distribution information of heatmap activation via Taylor-expansion based distribution approximation. Besides, we observe that the standard method for generating the ground-truth heatmaps suffers from *quantisation errors*, leading to imprecise supervision signals and inferior model performance. To solve this issue, we propose generating the *unbiased* heatmaps allowing Gaussian kernel being centred at sub-pixel locations.

Our **contribution** is that, we discover the previously unrealised significance of coordinate representation in human pose estimation, and propose a *Distribution-Aware coordinate Representation of Keypoints* (DARK) method with two key components: (1) efficient Taylor-expansion based coordinate decoding, and (2) unbiased sub-pixel centred coordinate encoding. Importantly, existing human pose methods can be seamlessly benefited from DARK *without* any algorithmic modification. Extensive experiments on two common benchmarks (MPII and COCO) show that our method provides significant performance improvement for existing state-of-the-art human pose estimation models [25, 33, 20], achieving the best single model accuracy on COCO and MPII. DARK favourably enables the use of smaller input image resolutions with much smaller performance degradation, whilst dramatically boosting the model inference efficiency therefore facilitating low-latency and low-energy applications as required in embedded AI scenarios.

2. Related Work

Generally, there are two common coordinate representation designs in human pose estimation: coordinate and heatmap. Both are used as the regression targets in existing methods, which will be reviewed separately in the follows.

Coordinate regression Directly taking the coordinates as model output target is straightforward and intuitive. But only a handful of existing methods adopt this design [31, 10, 3, 21, 27]. One plausible reason is that, this representation lacks the spatial and contextual information, making the learning of human pose model extremely challenging due to the intrinsic visual ambiguity in joint location.

Heatmap regression The heatmap representation elegantly addresses the above limitations. It was firstly introduced in [30] and rapidly became the most commonly used coordinate representation. Generally, the mainstream research focus is on designing network architectures for more effectively regressing the heatmap supervision. Representative design improvements include sequential modelling [12, 2], receptive field expansion [32], position voting [16], intermediate supervision [20, 32], pairwise relations modelling [4], tree structure modelling [8, 35, 7, 26, 29], hierarchical context learning [37], pyramid residual learning [34], cascaded pyramid learning [6], knowledge-guided learning [22], active learning [18], adversarial learning [5], deconvolution upsampling [33], multi-scale supervision [14], attentional mechanism [19, 24], and high-resolution representation preserving [25].

In contrast to all previous works, we instead investigate the issues of heatmap representation on human pose estimation, a largely ignored perspective in the literature. Not only do we reveal a big impact of resolution reduction in the process of using heatmap but also we propose a principled coordinate representation method for significantly improving the performance of existing models. Crucially, our method can be seamlessly integrated without model design change.

3. Methodology

We consider the coordinate representation problem including encoding and decoding in human pose estimation. The objective is to predict the joint coordinates in a given input image. To that end, we need to learn a regression model from the input image to the output coordinates, and the *heatmap* is often leveraged as coordinate representation during both model training and testing. Specifically, we assume access to a training set of images. To facilitate the model learning, we *encode* the labelled ground-truth coordinate of a joint into a heatmap as the learning target. In testing, we then need to *decode* the predicted heatmap into the coordinate in the original image coordinate space.

In the following we first describe the decoding process, focusing on the limitation analysis of the existing standard method and the development of a novel solution. Then, we further discuss and address the limitations of the encoding process. Lastly, we describe the integration of existing human pose estimation models with the proposed method.

3.1. Coordinate Decoding

Considered seemingly as an insignificant component of the model testing pipeline, as we will show, *coordinate decoding* turns out to be one of the most significant performance contributors. for human pose estimation (cf. Table 1). Specifically, it is a process of translating a predicted heatmap of each individual joint into a coordinate in the *original* image space. Suppose the heatmap has the same

spatial size as the original image, we only need to find the location of the maximal activation as the joint coordinate prediction. However, this is often not the case as interpreted above. Instead, we need to upsample the heatmaps to the original image resolution by a sample-specific unconstrained factor $\lambda \in \mathcal{R}_+$. This involves a *sub-pixel localisation* problem. Before introducing our method, we first revisit the standard coordinate decoding method used in existing pose estimation models.

The standard coordinate decoding method is designed empirically according to model performance [20]. Specifically, given a heatmap $\boldsymbol{h}$ predicted by a trained model, we first identify the coordinates of the maximal ($\boldsymbol{m}$) and second maximal ($\boldsymbol{s}$) activation. The joint location is then predicted as

$$\boldsymbol{p} = \boldsymbol{m} + 0.25 \frac{\boldsymbol{s} - \boldsymbol{m}}{\|\boldsymbol{s} - \boldsymbol{m}\|_2} \tag{1}$$

where $\|\cdot\|_2$ defines the magnitude of a vector. This means that the prediction is as the maximal activation with a 0.25 pixel (*i.e.* sub-pixel) shifting towards the second maximal activation in the heatmap space. The final coordinate prediction in the original image is computed as:

$$\hat{\boldsymbol{p}} = \lambda \boldsymbol{p} \tag{2}$$

where λ is the resolution reduction ratio.

Remarks The aim of the sub-pixel shifting in Eq. (1) is to compensate the quantisation effect of image resolution downsampling. That being said, the maximum activation in the predicted heatmap does not correspond to the accurate position of the joint in the original coordinate space, but only to a *coarse* location. As we will show, this shifting *surprisingly* brings a significant performance boost (Table 1). This may partly explain why it is often used as a standard operation in model test. Interestingly, to our best knowledge no specific work has delved into the effect of this operation on human pose estimation performance. Therefore, its true significance has never been really recognised and reported in the literature. While this standard method lacks intuition and interpretation in design, no dedicated investigation has been carried out for improvement. We fill this gap by presenting a principled method for shifting estimation and finally more accurate human pose estimation.

Our coordinate decoding method explores the distribution structure of the predicted heatmap to infer the underlying maximum activation. This differs dramatically to the standard method above relying on a hand-designed offset prediction, with little design justification and rationale.

Specifically, to obtain the accurate location at the degree of sub-pixel, we assume the predicted heatmap follows a 2D Gaussian distribution, same as the ground-truth heatmap.
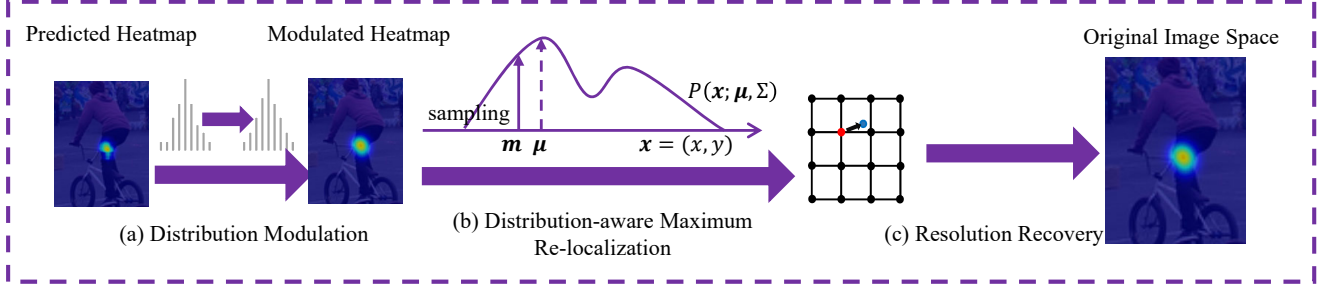
Figure 2. Overview of the proposed distribution aware coordinate decoding method.

Therefore, we represent the predicted heatmap as

$$\mathcal{G}(\boldsymbol{x};\boldsymbol{\mu},\Sigma) = \frac{1}{(2\pi)|\Sigma|^{\frac{1}{2}}} \exp\left(-\frac{1}{2}(\boldsymbol{x}-\boldsymbol{\mu})^T\Sigma^{-1}(\boldsymbol{x}-\boldsymbol{\mu})\right) \tag{3}$$

where $\boldsymbol{x}$ is a pixel location in the predicted heatmap, $\boldsymbol{\mu}$ is the Gaussian mean (centre) corresponding to the *to-be-estimated* joint location. The covariance Σ is a diagonal matrix, same as that used in coordinate encoding:

$$\Sigma = \begin{bmatrix} \sigma^2 & 0 \\ 0 & \sigma^2 \end{bmatrix} \tag{4}$$

where σ is the standard deviation same for both directions.

In order to reduce the approximation difficulty, we use *logarithm* to transform the original exponential form $\mathcal{G}$ to a quadratic form $\mathcal{P}$ to facilitate inference while keeping the original maximum activation location as:

$$\mathcal{P}(\boldsymbol{x};\boldsymbol{\mu},\Sigma) = \ln(\mathcal{G}) = -\ln(2\pi) - \frac{1}{2}\ln(|\Sigma|) \tag{5}$$
$$-\frac{1}{2}(\boldsymbol{x}-\boldsymbol{\mu})^T\Sigma^{-1}(\boldsymbol{x}-\boldsymbol{\mu})$$

Our objective is to estimate $\boldsymbol{\mu}$. As an extreme point in the distribution, it is well-known that the first derivative at the location $\boldsymbol{\mu}$ meets a condition as:

$$\mathcal{D}'(\boldsymbol{x})\Big|_{\boldsymbol{x}=\boldsymbol{\mu}} = \frac{\partial \mathcal{P}^T}{\partial \boldsymbol{x}}\Big|_{\boldsymbol{x}=\boldsymbol{\mu}} = -\Sigma^{-1}(\boldsymbol{x}-\boldsymbol{\mu})\Big|_{\boldsymbol{x}=\boldsymbol{\mu}} = 0 \tag{6}$$

To explore this condition, we adopt the Taylor's theorem. Formally, we approximate the activation $\mathcal{P}(\mu)$ by a Taylor series (up to the quadratic term) evaluated at the maximal activation $\boldsymbol{m}$ of the predicted heatmap as

$$\mathcal{P}(\boldsymbol{\mu}) = \mathcal{P}(\boldsymbol{m}) + \mathcal{D}'(\boldsymbol{m})(\boldsymbol{\mu}-\boldsymbol{m}) + \frac{1}{2}(\boldsymbol{\mu}-\boldsymbol{m})^T\mathcal{D}''(\boldsymbol{m})(\boldsymbol{\mu}-\boldsymbol{m}) \tag{7}$$

where $\mathcal{D}''(\boldsymbol{m})$ denotes the second derivative (*i.e.* Hessian) of $\mathcal{P}$ evaluated at $\boldsymbol{m}$, formally defined as:

$$\mathcal{D}''(\boldsymbol{m}) = \mathcal{D}''(\boldsymbol{x})\Big|_{\boldsymbol{x}=\boldsymbol{m}} = -\Sigma^{-1} \tag{8}$$

The intuition of selecting $\boldsymbol{m}$ to approximate $\boldsymbol{\mu}$ is that it represents a good coarse joint prediction that approaches $\boldsymbol{\mu}$.

Taking Eq. (6), (7), and (8) together, we finally obtain

$$\boldsymbol{\mu} = \boldsymbol{m} - \left(\mathcal{D}''(\boldsymbol{m})\right)^{-1}\mathcal{D}'(\boldsymbol{m}) \tag{9}$$

where $\mathcal{D}''(\boldsymbol{m})$ and $\mathcal{D}'(\boldsymbol{m})$ can be estimated efficiently from the heatmap. Once obtaining $\boldsymbol{\mu}$, we also apply Eq. (2) to predict the coordinate in the original image space.

Remarks In contrast to the standard method considering the second maximum activation alone in heatmap, the proposed coordinate decoding fully explores the heatmap distributional statistics for revealing the underlying maximum more accurately. In theory, our method is based on a principled distribution approximation under a training-supervision-consistent assumption that the heatmap is in a Gaussian distribution. Crucially, it is very efficient computationally as it only needs to compute the first and second derivative of **one pixel location** per heatmap. Consequently, existing human pose estimation approaches can be readily benefited without any computational cost barriers.

Heatmap distribution modulation As the proposed coordinate decoding method is based on a Gaussian distribution assumption, it is necessary for us to examine how well this condition is satisfied. We found that, often, the heatmaps predicted by a human pose estimation model do *not* exhibit good-shaped Gaussian structure compared to the training heatmap data. As shown in Fig. 3(a), the heatmap usually presents multiple peaks around the maximum activation. This may cause negative effects to the performance of our decoding method. To address this issue, we propose *modulating* the heatmap distribution beforehand.

Specifically, to match the requirement of our method we propose exploiting a Gaussian kernel K with the same variation as the training data to smooth out the effects of multiple peaks in the heatmap $\boldsymbol{h}$, formally as

$$\boldsymbol{h}' = K \circledast \boldsymbol{h} \tag{10}$$

where $\circledast$ specifies the convolution operation.

To preserve the original heatmap's magnitude, we finally scale $\boldsymbol{h}'$ so that its maximum activation is equal to that of

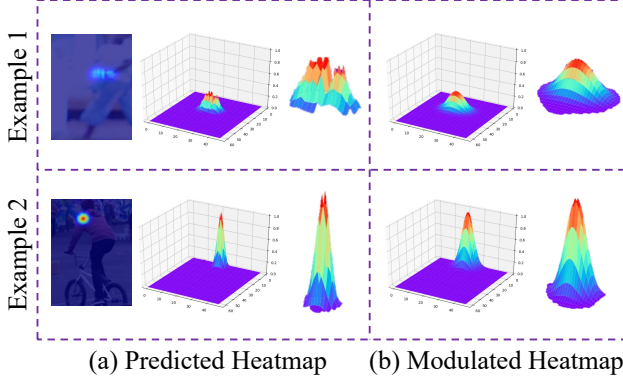(a) Predicted Heatmap   (b) Modulated Heatmap

Figure 3. Illustration of heatmap distribution modulation. (a) Predicted heatmap; (b) Modulated heatmap distribution.
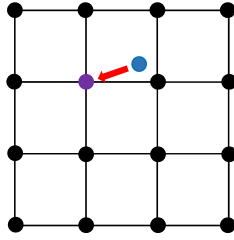

Figure 4. Illustration of quantisation error in the standard coordinate encoding process. The blue point denotes the accurate position (g') of a joint. With the *floor* based coordinate quantisation, an error (indicated by red arrow) is introduced. Other quantisation methods share the same problem.

h, via the following transformation:

$$h' = \frac{h' - \min(h')}{\max(h') - \min(h')} * \max(h) \quad (11)$$

where $\max()$ and $\min()$ return the maximum and minimum values of an input matrix, respectively. In our experimental analysis, it is validated that this distribution modulation further improves the performance of our coordinate decoding method (Table 3), with the resulting visual effect and qualitative evaluation demonstrated in Fig. 3(b).

Summary We summarise our coordinate decoding method in Fig. 2. Specifically, a total of three steps are involved in a sequence: **(a)** Heatmap distribution modulation (Eq. (10), (11)), **(b)** Distribution-aware joint localisation by Taylor expansion at sub-pixel accuracy (Eq. (3)-(9)), **(c)** Resolution recovery to the original coordinate space (Eq. (2)). None of these steps incur high computational costs, therefore being able to serve as an efficient plug-in for existing models.

3.2. Coordinate Encoding

The previous section has addressed the problem with coordinate decoding, rooted at resolution reduction. Coordinate encoding also shares the same limitation. Specifically, the standard coordinate encoding method starts with

downsampling original person images into the model input size. So, the ground-truth joint coordinates need to be transformed accordingly before generating the heatmaps.

Formally, we denote by $g = (u, v)$ the ground-truth coordinate of a joint. The resolution reduction is defined as:

$$g' = (u', v') = \frac{g}{\lambda} = \left(\frac{u}{\lambda}, \frac{v}{\lambda}\right) \quad (12)$$

where λ is the downsampling ratio.

Conventionally, for facilitating the kernel generation, we often quantise g':

$$g'' = (u'', v'') = \text{quantise}(g') = \text{quantise}\left(\frac{u}{\lambda}, \frac{v}{\lambda}\right) \quad (13)$$

where quantise() specifies a quantisation function, with the common choices including floor, ceil and round.

Subsequently, the heatmap centred at the quantised coordinate g'' can be synthesised through:

$$\mathcal{G}(x, y; g'') = \frac{1}{2\pi\sigma^2} \exp\left(-\frac{(x - u'')^2 + (y - v'')^2}{2\sigma^2}\right) \quad (14)$$

where (x, y) specifies a pixel location in the heatmap, and σ denotes a fixed spatial variance.

Obviously, the heatmaps generated in the above way are *inaccurate* and *biased* due to the quantisation error (Fig. 4). This may introduce sub-optimal supervision signals and result in degraded model performance, particularly for accurate coordinate encoding as proposed in this work.

To address this issue, we simply place the heatmap centre at the non-quantised location g' which represents the *accurate* ground-truth coordinate. We still apply Eq. (14) but replacing g'' with g'. We will demonstrate the benefits of this *unbiased* heatmap generation method (Table 3).

3.3. Integration with State-of-the-Art Models

DARK is model-agnostic, seamlessly integrable with any existing heatmap based pose models. Importantly, this does not involve any algorithmic changes to previous methods. In particular, during training the only change is the ground-truth heatmap data generated based on the accurate joint coordinates. At test time, we take as input the predicted heatmaps predicted by any model such as HRNet [25], and output more accurate joint coordinates in the original image space. In the whole lifecycle, we keep an existing model intact as the original design. This allows to maximise the generality and scalability of our method.

4. Experiments

Datasets We used two popular human pose estimation datasets, COCO and MPII. The ***COCO*** keypoint dataset [17] presents naturally challenging imagery data with various human poses, unconstrained environments, different body scales and occlusion patterns. The entire objective

Decoding	AP	AP^{50}	AP^{75}	AP^M	AP^L	AR
No Shifting	61.2	88.1	72.3	59.0	66.3	68.7
Standard Shifting	66.9	**88.7**	76.3	64.6	72.3	73.7
Ours	**68.4**	88.6	**77.4**	**66.0**	**74.0**	**74.9**

Table 1. Effect of coordinate decoding on the COCO validation set. Model: HRNet-W32; Input size: 128×96.

involves both detecting person instances and localising the body joints. It contains 200,000 images and 250,000 person samples. Each person instance is labelled with 17 joints. The annotations of training and validation sets are publicly benchmarked. In evaluation, we followed the commonly used train2017/val2017/test-dev2017 split. The *MPII* human pose dataset [1] contains 40k person samples, each labelled with 16 joints. We followed the standard train/val/test split as in [30].

Evaluation metrics We used Object Keypoint Similarity (OKS) for COCO and Percentage of Correct Keypoints (PCK) for MPII to evaluate the model performance.

Implementation details For model training, we used the Adam optimiser. For HRNet [25] and SimpleBaseline [33], we followed the same learning schedule and epochs as in the original works. For Hourglass [20], the base learning rate was fine-tuned to 2.5e-4, and decayed to 2.5e-5 and 2.5e-6 at the 90-th and 120-th epoch. The total number of epochs is 140. We used three different input sizes (128×96, 256×192, 384×288) in our experiments. We adopted the same data preprocessing as in [25].

DM	AP	AP^{50}	AP^{75}	AP^M	AP^L	AR
✗	68.1	88.5	77.1	65.8	73.7	74.8
✓	**68.4**	**88.6**	**77.4**	**66.0**	**74.0**	**74.9**

Table 2. Effect of distribution modulation (DM) on the COCO val set. Backbone: HRNet-W32; Input size: 128×96.

4.1. Evaluating Coordinate Representation

As the core problem in this work, the effect of coordinate representation on model performance was firstly examined, with a connection to the input image resolution (size). In this test, by default we used HRNet-W32 [25] as the backbone model and 128×96 as the input size, and reported the accuracy results on the COCO validation set.

Encode	Decode	AP	AP^{50}	AP^{75}	AP^M	AP^L	AR
Biased	Standard	66.9	88.7	76.3	64.6	72.3	73.7
Unbiased	Standard	**68.0**	**88.9**	**77.0**	**65.4**	**73.7**	**74.5**
Biased	**Ours**	68.4	88.6	77.4	66.0	74.0	74.9
Unbiased	**Ours**	**70.7**	**88.9**	**78.4**	**67.9**	**76.6**	**76.7**

Table 3. Effect of coordinate encoding on the COCO validation set. Model: HRNet-W32; Input size: 128×96.

Method	Input size	GFLOPs	AP	AP^{50}	AP^{75}	AP^M	AP^L	AR
HRN32	128×96	1.8	66.9	88.7	76.3	64.6	72.3	73.7
DARK			**70.7**	**88.9**	**78.4**	**67.9**	**76.6**	**76.7**
HRN32	256×192	7.1	74.4	90.5	81.9	70.8	81.0	79.8
DARK			**75.6**	**90.5**	**82.1**	**71.8**	**82.8**	**80.8**
HRN32	384×288	16.0	75.8	90.6	82.5	72.0	82.7	80.9
DARK			**76.6**	**90.7**	**82.8**	**72.7**	**83.9**	**81.5**

Table 4. Effect of input image size on the COCO validation set. DARK uses HRNet-W32 (HRN32) as backbone.

Figure 5. Examples by DARK (red) *vs.* HRNet-W32 (cyan).

(i) Coordinate decoding We evaluated the effect of coordinate decoding, in particular, the shifting operation and distribution modulation. The conventional biased heatmaps were used. In this test, we compared the proposed distribution-aware shifting method with *no shifting* (*i.e.* directly using the maximal activation location), and the *standard shifting* (Eq. (1)). We make two major observations in Table 1: **(i)** The standard shifting gives as high as 5.7% AP accuracy boost, which is surprisingly effective. To our best knowledge, this is the first reported effectiveness analysis in the literature, since this problem is largely ignored by previous studies. This reveals previously unseen significance of coordinate decoding to human pose estimation. **(ii)** Despite the great gain by the standard decoding method, the proposed model further improves AP score by 1.5%, among which the distribution modulation gives 0.3% as shown in Table 2. This validates the superiority of our decoding method.

(ii) Coordinate encoding We tested how effective coordinate encoding can be. We compared the proposed *unbiased* encoding with the standard *biased* encoding, along with both the standard and our decoding method. We observed from Table 3 that our unbiased encoding with accurate kernel centre brings positive performance margin, regardless of the coordinate decoding method. In particular, unbiased encoding contributes consistently over 1% AP gain in both cases. This suggests the importance of coordinate encoding, which again is neglected by previous investigations.

DARK	Baseline	Input size	#Params	GFLOPs	AP	AP^{50}	AP^{75}	AP^{M}	AP^{L}	AR
✗	Hourglass (4 Blocks)	128×96	13.0M	2.7	66.2	87.6	75.1	63.8	71.4	72.8
✓					**69.6**	**87.8**	**77.0**	**67.0**	**75.4**	**75.7**
✗	Hourglass (8 Blocks)	128×96	25.1M	4.9	67.6	**88.3**	77.4	65.2	73.0	74.0
✓					**70.8**	87.9	**78.3**	**68.3**	**76.4**	**76.6**
✗	SimpleBaseline-R50	128×96	34.0M	2.3	59.3	85.5	67.4	57.8	63.8	66.6
✓					**62.6**	**86.1**	**70.4**	**60.4**	**67.9**	**69.5**
✗	SimpleBaseline-R101	128×96	53.0M	3.1	58.8	85.3	66.1	57.3	63.4	66.1
✓					**63.2**	**86.2**	**71.1**	**61.2**	**68.5**	**70.0**
✗	SimpleBaseline-R152	128×96	68.6M	3.9	60.7	86.0	69.6	59.0	65.4	68.0
✓					**63.1**	**86.2**	**71.6**	**61.3**	**68.1**	**70.0**
✗	HRNet-W32	128×96	28.5M	1.8	66.9	88.7	76.3	64.6	72.3	73.7
✓					**70.7**	**88.9**	**78.4**	**67.9**	**76.6**	**76.7**
✗	HRNet-W48	128×96	63.6M	3.6	68.0	88.9	77.4	65.7	73.7	74.7
✓					**71.9**	**89.1**	**79.6**	**69.2**	**78.0**	**77.9**

Table 5. Evaluating the generality of our DARK method to varying state-of-the-art models on the COCO validation set.

Method	AP	AP^{50}	AP^{75}	AP^{M}	AP^{L}	AR
DSNT [21]	57.6	83.5	63.1	56.9	60.1	71.2
IPR [27]	68.0	88.1	76.5	65.9	73.8	74.4
DARK	**70.7**	**88.9**	**78.4**	**67.9**	**76.6**	**76.7**

Table 6. Comparing coordinate regression methods on the COCO validation set. Backbone: HRNet-W32; Input size: 128×96.

(iii) Input resolution We examined the impact of input image resolution/size by testing a number of different sizes, considering that it is an important factor relevant to model inference efficiency. We compared our DARK model (HRNet-W32 as backbone) with the original HRNet-W32 using the biased heatmap supervision for training and the standard shifting for testing. From Table 4 we have a couple of observations: **(a)** With reduced input image size, as expected the model performance consistently degrades whilst the inference cost drops clearly. **(b)** With the support of DARK, the model performance loss can be effectively mitigated, especially in case of very small input resolution (*i.e.* very fast model inference). This facilitates the deployment of human pose estimation models on low-resource devices, highly desired in the emerging embedded AI.

(iv) Generality Besides the state-of-the-art HRNet, we also tested other two representative human pose estimation models under varying CNN architectures: SimpleBaseline [33] and Hourglass [20]. The results in Table 5 show that DARK provides significant performance gain to the existing models in most cases. This suggests a generic usefulness of our approach. We showed qualitative evaluation in Fig. 5.

(v) Complexity We tested the inference efficiency impact by our method in HRNet-W32 at input size of 128×96. On a machine with one i9-7920X CPU and one Titan V GPU, the running speed is reduced from 360 fps to 320 fps

in the *low-efficient* python environment, *i.e.* a drop of 11%. Hence, the extra cost from DARK is rather affordable. We believe a native programming language (e.g. C/C++) based version can further accelerate the inference speed.

4.2. Comparison to Coordinate Regression

We compared our DARK with existing coordinate regression methods including IPR [27] and DSNT [21]. In this test, we used HRNet-W32 [25] as the backbone and 128 × 96 as the input size, and reported the accuracy results on the COCO validation set. Table 6 verifies the performance superiority of our method over both alternatives, whilst enjoying the advantages of more friendly adoption and more efficient model training.

4.3. Comparison to State-of-the-Art Methods

(i) Evaluation on COCO We compared our DARK method with top-performers including G-RMI [23], IPR [27], CPN [6], CFN [13] RMPE [11], SimpleBaseline [33], and HRNet [25]. Table 7 shows the accuracy results of the state-of-the-art methods and DARK on the COCO test-dev set. In this test, we used the person detection results from [25]. We have the following observations: **(i)** DARK with HRNet-W48 at the input size of 384×288 achieves the best accuracy, without extra model parameters and only tiny cost increase. Specifically, compared with the best competitor (HRNet-W48 with the same input size), DARK further improves AP by 0.7% (76.2-75.5). When compared to the most efficient model (IPR), DARK(HRNet-W32) achieves an AP gain of 2.2% (70.0-67.8) whilst only needing 16.4% (1.8/11.0 GFLOPs) execution cost. These suggest the advantages and flexibility of DARK on top of existing models in terms of both accuracy and efficiency.

Method	Backbone	Input size	#Params	GFLOPs	AP	AP^{50}	AP^{75}	AP^M	AP^L	AR
G-RMI[23]	ResNet-101	353×257	42.6M	57.0	64.9	85.5	71.3	62.3	70.0	69.7
IPR [27]	ResNet-101	256×256	45.1M	11.0	67.8	88.2	74.8	63.9	74.0	-
CPN [6]	ResNet-Inception	384×288	-	-	72.1	91.4	80.0	68.7	77.2	78.5
RMPE [11]	PyraNet	320×256	28.1M	26.7	72.3	89.2	79.1	68.0	78.6	-
CFN [13]	-	-	-	-	72.6	86.1	69.7	78.3	64.1	-
CPN (ensemble) [6]	ResNet-Inception	384×288	-	-	73.0	91.7	80.9	69.5	78.1	79.0
SimpleBaseline[33]	ResNet-152	384×288	68.6M	35.6	73.7	91.9	81.1	70.3	80.0	79.0
HRNet[25]	HRNet-W32	384×288	28.5M	16.0	74.9	**92.5**	82.8	71.3	80.9	80.1
HRNet[25]	HRNet-W48	384×288	63.6M	32.9	75.5	**92.5**	83.3	71.9	81.5	80.5
DARK	HRNet-W32	128×96	28.5M	**1.8**	70.0	90.9	78.5	67.4	75.0	75.9
DARK	HRNet-W48	384×288	63.6M	32.9	**76.2**	**92.5**	**83.6**	**72.5**	**82.4**	**81.1**
G-RMI (extra data)	ResNet-101	353×257	42.6M	57.0	68.5	87.1	75.5	65.8	73.3	73.3
HRNet (extra data)	HRNet-W48	384×288	63.6M	32.9	77.0	**92.7**	84.5	73.4	83.1	82.0
DARK (extra data)	HRNet-W48	384×288	63.6M	32.9	**77.4**	92.6	**84.6**	**73.6**	**83.7**	**82.3**

Table 7. Comparison with the state-of-the-art human pose estimation methods on the COCO test-dev set.

Method	Head	Sho.	Elb.	Wri.	Hip	Kne.	Ank.	Mean
PCKh@0.5								
HRN32	97.1	**95.9**	90.3	86.5	89.1	**87.1**	83.3	90.3
DARK	**97.2**	**95.9**	**91.2**	**86.7**	**89.7**	86.7	**84.0**	**90.6**
PCKh@0.1								
HRN32	51.1	42.7	42.0	41.6	17.9	29.9	31.0	37.7
DARK	**55.2**	**47.8**	**47.4**	**45.2**	**20.1**	**33.4**	**35.4**	**42.0**

Table 8. Comparison on the MPII validation set. DARK uses HRNet-W32 (HRN32) as backbone. Input size: 256×256. Single-scale model performance is considered.

AP	AP^{50}	AP^{75}	AP^M	AP^L	AR
test-dev					
78.9	93.8	86.0	75.1	84.4	83.5
test-challenge					
76.4	92.5	82.7	70.9	83.8	81.6

Table 9. The results of our DARK based entry in the ICCV2019 COCO Keypoints Challenge.

(ii) Evaluation on MPII We compared DARK with HRNet-W32 on the MPII validation set. The comparisons in Table 8 show a consistent performance superiority of our method over the best competitor. Under the more strict accuracy measurement PCKh@0.1, the performance margin of DARK is even more significant. Note, MPII provides significantly smaller training data than COCO, suggesting that our method generalises across varying training data sizes.

4.4. COCO Keypoints Detection Challenge

We participated in the ICCV 2019 COCO Keypoints Challenge using the proposed DARK as the main method. To push up the performance, we used an ensemble of DARK models. Table 9 shows that our method achieves 78.9% AP on test-dev set and 76.4% AP on test-challenge set for multi-person pose estimation. This enables us to achieve the 2nd place entry in this Challenge. For more details, we refer the readers to our technique report [9].

5. Conclusion

We for the first time systematically investigated the largely ignored yet significant problem of *coordinate representation* (including encoding and decoding) for human pose estimation in unconstrained images. We not only revealed the genuine significance of this problem, but also presented a novel distribution-aware coordinate representation (DARK) for more discriminative model training and inference. Serving as a ready-to-use plug-in component, existing state-of-the-art models can be seamlessly benefited from our DARK method without any algorithmic adaptation at a neglectable cost. Apart from demonstrating empirically the importance of coordinate representation, we validated the performance advantages of DARK by conducting extensive experiments with a wide spectrum of contemporary models on two challenging datasets. We also provided a sequence of in-depth component analysis for giving insights on the design rationale of our model formulation.

References

[1] Mykhaylo Andriluka, Leonid Pishchulin, Peter Gehler, and Bernt Schiele. 2d human pose estimation: New benchmark and state of the art analysis. In *IEEE Conference on Computer Vision and Pattern Recognition*, 2014.

[2] Vasileios Belagiannis and Andrew Zisserman. Recurrent human pose estimation. In *IEEE Conference on Automatic Face and Gesture Recognition*, 2017.

[3] Joao Carreira, Pulkit Agrawal, Katerina Fragkiadaki, and Jitendra Malik. Human pose estimation with iterative error feedback. In *IEEE Conference on Computer Vision and Pattern Recognition*, 2016.

[4] Xianjie Chen and Alan L Yuille. Articulated pose estimation by a graphical model with image dependent pairwise relations. In *Advances in Neural Information Processing Systems*, 2014.

[5] Yu Chen, Chunhua Shen, Xiu-Shen Wei, Lingqiao Liu, and Jian Yang. Adversarial posenet: A structure-aware convolutional network for human pose estimation. In *IEEE International Conference on Computer Vision*, 2017.

[6] Yilun Chen, Zhicheng Wang, Yuxiang Peng, Zhiqiang Zhang, Gang Yu, and Jian Sun. Cascaded pyramid network for multi-person pose estimation. In *IEEE Conference on Computer Vision and Pattern Recognition*, June 2018.

[7] Xiao Chu, Wanli Ouyang, Hongsheng Li, and Xiaogang Wang. Structured feature learning for pose estimation. In *IEEE Conference on Computer Vision and Pattern Recognition*, 2016.

[8] Xiao Chu, Wanli Ouyang, Xiaogang Wang, et al. Crf-cnn: Modeling structured information in human pose estimation. In *Advances in Neural Information Processing Systems*, pages 316–324, 2016.

[9] Hanbin Dai, Liangbo Zhou, Feng Zhang, Zhengyu Zhang, Hong Hu, Xiatian Zhu, and Mao Ye. Joint coco and mapillary workshop at iccv 2019 keypoint detection challenge track technical report: Distribution-aware coordinate representation for human pose estimation. *arXiv e-print*, 2020.

[10] Xiaochuan Fan, Kang Zheng, Yuewei Lin, and Song Wang. Combining local appearance and holistic view: Dual-source deep neural networks for human pose estimation. In *IEEE Conference on Computer Vision and Pattern Recognition*, 2015.

[11] Hao-Shu Fang, Shuqin Xie, Yu-Wing Tai, and Cewu Lu. Rmpe: Regional multi-person pose estimation. In *IEEE Conference on Computer Vision and Pattern Recognition*, pages 2334–2343, 2017.

[12] Georgia Gkioxari, Alexander Toshev, and Navdeep Jaitly. Chained predictions using convolutional neural networks. In *European Conference on Computer Vision*, 2016.

[13] Shaoli Huang, Mingming Gong, and Dacheng Tao. A coarse-fine network for keypoint localization. In *IEEE International Conference on Computer Vision*, pages 3028–3037, 2017.

[14] Lipeng Ke, Ming-Ching Chang, Honggang Qi, and Siwei Lyu. Multi-scale structure-aware network for human pose estimation. In *European Conference on Computer Vision*, September 2018.

[15] Yann LeCun, Léon Bottou, Yoshua Bengio, Patrick Haffner, et al. Gradient-based learning applied to document recognition. *Proceedings of the IEEE*, 86(11):2278–2324, 1998.

[16] Ita Lifshitz, Ethan Fetaya, and Shimon Ullman. Human pose estimation using deep consensus voting. *European Conference on Computer Vision*, 2016.

[17] Tsung-Yi Lin, Michael Maire, Serge Belongie, James Hays, Pietro Perona, Deva Ramanan, Piotr Dollár, and C Lawrence Zitnick. Microsoft coco: Common objects in context. In *European Conference on Computer Vision*, 2014.

[18] Buyu Liu and Vittorio Ferrari. Active learning for human pose estimation. In *IEEE International Conference on Computer Vision*, pages 4363–4372, 2017.

[19] Wentao Liu, Jie Chen, Cheng Li, Chen Qian, Xiao Chu, and Xiaolin Hu. A cascaded inception of inception network with attention modulated feature fusion for human pose estimation. In *AAAI Conference on Artificial Intelligence*, 2018.

[20] Alejandro Newell, Kaiyu Yang, and Jia Deng. Stacked hourglass networks for human pose estimation. In *European Conference on Computer Vision*, 2016.

[21] Aiden Nibali, Zhen He, Stuart Morgan, and Luke Prendergast. Numerical coordinate regression with convolutional neural networks. *arXiv preprint arXiv:1801.07372*, 2018.

[22] G. Ning, Z. Zhang, and Z. He. Knowledge-guided deep fractal neural networks for human pose estimation. *IEEE Transactions on Multimedia*, PP(99):1–1, 2017.

[23] George Papandreou, Tyler Zhu, Nori Kanazawa, Alexander Toshev, Jonathan Tompson, Chris Bregler, and Kevin Murphy. Towards accurate multi-person pose estimation in the wild. In *IEEE Conference on Computer Vision and Pattern Recognition*, pages 4903–4911, 2017.

[24] Kai Su, Dongdong Yu, Zhenqi Xu, Xin Geng, and Changhu Wang. Multi-person pose estimation with enhanced channel-wise and spatial information. In *IEEE Conference on Computer Vision and Pattern Recognition*, June 2019.

[25] Ke Sun, Bin Xiao, Dong Liu, and Jingdong Wang. Deep high-resolution representation learning for human pose estimation. In *IEEE Conference on Computer Vision and Pattern Recognition*, 2019.

[26] Xiao Sun, Jiaxiang Shang, Shuang Liang, and Yichen Wei. Compositional human pose regression. In *IEEE International Conference on Computer Vision*, 2017.

[27] Xiao Sun, Bin Xiao, Fangyin Wei, Shuang Liang, and Yichen Wei. Integral human pose regression. In *European Conference on Computer Vision*, September 2018.

[28] Christian Szegedy, Vincent Vanhoucke, Sergey Ioffe, Jon Shlens, and Zbigniew Wojna. Rethinking the inception architecture for computer vision. In *IEEE Conference on Computer Vision and Pattern Recognition*, pages 2818–2826, 2016.

[29] Wei Tang, Pei Yu, and Ying Wu. Deeply learned compositional models for human pose estimation. In *European Conference on Computer Vision*, September 2018.

[30] Jonathan J Tompson, Arjun Jain, Yann LeCun, and Christoph Bregler. Joint training of a convolutional network and a graphical model for human pose estimation. In *Advances in Neural Information Processing Systems*, 2014.

[31] Alexander Toshev and Christian Szegedy. Deeppose: Human pose estimation via deep neural networks. In *IEEE Conference on Computer Vision and Pattern Recognition*, 2014.

[32] Shih-En Wei, Varun Ramakrishna, Takeo Kanade, and Yaser Sheikh. Convolutional pose machines. In *IEEE Conference on Computer Vision and Pattern Recognition*, 2016.

[33] Bin Xiao, Haiping Wu, and Yichen Wei. Simple baselines for human pose estimation and tracking. In *European Conference on Computer Vision*, 2018.

[34] Wei Yang, Shuang Li, Wanli Ouyang, Hongsheng Li, and Xiaogang Wang. Learning feature pyramids for human pose estimation. In *IEEE International Conference on Computer Vision*, 2017.

[35] Wei Yang, Wanli Ouyang, Hongsheng Li, and Xiaogang Wang. End-to-end learning of deformable mixture of parts and deep convolutional neural networks for human pose estimation. In *IEEE Conference on Computer Vision and Pattern Recognition*, 2016.

[36] Feng Zhang, Xiatian Zhu, Hanbin Dai, Mao Ye, and Ce Zhu. Distribution-aware coordinate representation for human pose estimation (code). `https://github.com/ilovepose/DarkPose`, 2020.

[37] Feng Zhang, Xiatian Zhu, and Mao Ye. Efficient human pose estimation in hierarchical context. *IEEE Access*, 7:29365–29373, 2019.

[38] Feng Zhang, Xiatian Zhu, and Mao Ye. Fast human pose estimation. In *IEEE Conference on Computer Vision and Pattern Recognition*, June 2019.